18TH WORLD CONFERENCE ON EARTHQUAKE ENGINEERING
WCEE2024
MILAN

MILAN, ITALY
30TH JUNE - 5TH JULY 2024
www.wcee2024.it

MODEL-BASED UNCERTAINTY IN PREDICTING DAMAGE TO NEAR-FAULT REINFORCED CONCRETE STRUCTURES

M. Kenawy[1] & B. Giffin[2]

[1] Oklahoma State University, Stillwater, USA, mkenawy@okstate.edu

[2] Oklahoma State University, Stillwater, USA

Abstract: *Earthquake-induced ground shaking near rupturing faults typically contains strong velocity pulses dictated by the fault rupture characteristics and seismic wave propagation patterns, and can cause significant damage to civil structures compared to ground shaking at locations further away from the fault. Therefore, modeling of the nonlinear, and especially degrading, behavior of near-fault structures with a high degree of fidelity is important for evaluating the structural demands in geographical regions proximate to active faults. Several alternative modeling strategies of varying fidelities exist for representing damage mechanisms in structures under dynamic earthquake loading, but it remains unclear the extent to which the specific choice of modeling strategy affects the estimated risks to near-fault structures. In this study, we examine the bias associated with the predicted seismic demands on near-fault reinforced concrete structures due to deficiencies in the modeling of the degrading behavior of the structural components. We test the use of three different modeling approaches which represent the deterioration of the structural components in different ways: (1) a lumped-plasticity frame model which cumulatively represents several damage mechanisms using nonlinear springs at the ends of the structural components, (2) a conventional distributed-plasticity frame model which represents the deterioration of the concrete and steel materials using uniaxial constitutive models, but is subject to numerical singularities, and (3) a regularized distributed-plasticity frame model recently developed by the authors which utilizes a nonlocal damage technique to overcome artificial strain singularities in representing the deterioration of the concrete and steel materials. We conduct a series of nonlinear dynamic analyses to predict the seismic demands imposed by representative ensembles of near-fault ground motions on structures located between 1 and 15 km away from the fault, and we compare the statistical distributions of the demands associated with each damage modeling approach. The findings of this study highlight the advantages and deficiencies of the different structural modeling strategies in the seismic analysis of degrading systems, and will aid in quantifying the modeling uncertainty associated with performance-based design of near-fault structures.*

1 Introduction

Earthquake-induced ground shaking near rupturing faults is typically characterized by high intensity and strong velocity pulses dictated by the fault rupture characteristics and seismic wave propagation patterns, and can cause significant damage to civil structures, compared to ground shaking at locations further away from the fault (Bertero et al. 1978, Hall et al. 1995, Champion and Liel 2012, Kenawy et al. 2021). Consequently, reliable modeling of the nonlinear, and especially degrading, behavior of near-fault structures with a high degree of fidelity is critical for evaluating the seismic structural demands in geographical regions proximate to active faults capable of large-magnitude earthquakes. A major challenge in evaluating the response of structural systems to strong ground shaking is the uncertainty associated with predicting extreme limit states induced by the deterioration of the structural components under dynamic loading conditions. This is especially important in setting the performance acceptance criteria in prescriptive or performance-based seismic design contexts.

For example, generic structural fragility functions are used to estimate a target risk of collapse in the seismic design of buildings (e.g., 1% probability of collapse in 50 years). However, all else being equal, the estimated risk of collapse using a numerical simulation may vary substantially depending on the approach used to model the damage mechanisms in the structural components (this is referred to as the modelling uncertainty). This uncertainty may be particularly influential for near-fault structures, because recent studies have found that the risk of collapse to structures evaluated using a dataset of near-fault ground motions was higher than the risk associated with the same systems evaluated using a far-field ground motion dataset (FEMA P-695, ATC 2009). Although the results of the FEMA P-695 study are useful in a relative sense, higher fidelity approaches to estimating the collapse capacity of structures may improve the predictions of the performance of near-fault structures, and support the evaluation of seismic response coefficients for existing and new structural systems.

Simulations of structural collapse conventionally use a lumped-plasticity (LP) modelling approach (Giberson 1967), in which the development of plastic hinges is assumed to occur at pre-determined locations at the structural member ends, whereas the rest of the member is assumed to behave elastically. In this type of model, a moment-rotation spring at the member ends is used to represent the nonlinear phenomena, including the progression of all localized degradation effects. For example, the deterioration of reinforced concrete (RC) structures is the result of localized nonlinear phenomena such as concrete crushing, confinement tie yielding and steel rebar buckling. LP models cumulatively represent such effects in a constitutive moment-rotation relationship that is empirically calibrated under certain loading cases (typically, quasi-static loading cycles). Although LP models are simple and computationally efficient, they require component-specific calibrations based on experimental test data, and cannot effectively capture the interaction between the axial load and bending moment in a structural member. In addition, because the plastic hinge locations are pre-determined, these models cannot capture the spread of damage along the structural member. Further, calibrations of the constitutive parameters are often based on simplified loading protocols that may not represent the behavior of the structural components under extreme dynamic loading conditions. Finally, applying structural damping effects in LP models can cause numerical issues and lead to spurious damping forces (Chopra and McKenna 2016).

Another type of model that is common in structural simulations is the distributed-plasticity fiber-section (DP) model, in which the nonlinear behavior of a structural component is determined by integrating the behavior at discrete locations (or fibers) and at multiple cross-sections (or integration points) along the member. The cross-sectional response resultants (generalized forces and deformations) are aggregated based on uniaxial constitutive relationships for the different materials in the cross section (e.g., unconfined concrete, confined concrete and steel, in the case of RC components). The DP modeling approach can capture the interaction of axial forces and bending moments in structural components, and simulate the initiation and propagation of plasticity along the member. However, in the context of collapse simulations, DP models fail to properly predict the strength degradation in the structural components (Coleman and Spacone 2001). This is due to the ill-posedness of boundary value problems involving strain-softening materials, which manifests as spurious mesh-dependent strain localization within a finite element (FE) analysis (Bažant and Belytschko 1985, Bažant and Lin 1988). More specifically, in a boundary value problem with a strain-softening material, the softening behavior will localize within a sub-domain of zero measure (e.g., a point in a one-dimensional model) within which the localized strain becomes infinite, and the dissipated energy vanishes. In a FE model, these characteristics lead to pathological sensitivity of the numerical solution to the chosen FE mesh size, such that the strain-softening zone tends to localize within a single element as the mesh is refined. This introduces an artificial dependence on the size of the FE elements used in the model, which is not physically meaningful.

Remedies to this problem emerged in the past few decades by introducing an auxiliary length parameter to control the size of the strain-softening zone in a numerical FE model, thereby alleviating the pathological solution sensitivity to the mesh size. A widely established and robust method to regularize the softening problem in this fashion is the nonlocal continuum theory (Bažant and Jirásek 2002), in which spatial interactions are introduced between neighboring locations within a chosen length scale in the model. DP frame elements that follow the nonlocal theory or a variation thereof have been proposed by several researchers in recent years (e.g., Sideris and Salehi 2016, Kenawy et al. 2018, Feng et al. 2023). The nonlocal (or regularized) DP models circumvent many of the limitations of the LP models, and may offer a viable approach for simulating the failure behavior of RC structures.

The purpose of this study is to assess the sensitivity of the predicted extreme limit states in a RC structural component to the modeling approach, in a dynamic analysis context under the influence of strong near-fault ground shaking. We start by describing a nonlocal frame element and constitutive model for concrete which was developed by the first author, and proceed to present a new nonlocal constitutive model which represents the buckling of steel rebar. Using these models, we study the demands on a RC column imposed by near-fault earthquake ground motions, and compare them against the demands predicted by the LP model, and a conventional (non-regularized or local) version of the DP model. We use all three models to study the sensitivity of the predicted collapse fragility of the column to the model type.

2 Structural Models and Study Design

The structural system of interest is a scale model of a cantilever RC column subjected to compressive axial force. The physical properties of the column match those of a laboratory test conducted by Soesianawati et al. (1986), such that the simulated behavior of the column can be compared to the behavior recorded in the experiment under quasi-static lateral loading conditions. The column specimen has a square cross section of 400 mm by 400 mm, and its effective inflection length is 1600 mm. The strength of the concrete in the column is 44 MPa, and the cross section is reinforced with 12 longitudinal steel bars (yield stress of 446 MPa), and transverse steel ties (yield stress of 360 MPa) spaced at 78 mm. The column is simulated using three different numerical models: (1) a LP frame model, (2) a conventional fiber-based DP frame model (referred to as the local model), and (3) a regularized nonlocal fiber-based DP frame model developed by the authors. All models were created using the structural analysis software OpenSees (McKenna et al. 2000).

In the LP model, the modified Ibarra-Medina-Krawinkler material model with peak-oriented hysteretic response (Ibarra et al. 2005) is used to represent the constitutive behavior of the nonlinear springs, and the model parameters are calibrated using the equations developed by Haselton et al. (2016). Further details about the LP simulation models are available in Kenawy et al. (2021) and Kenawy and McCallen (2021). The calibration of the DP models is straightforward, because the parameters controlling the elastic behavior of the concrete and steel materials are readily available in Soesianawati et al. (1986). The concepts underlying the nonlocal DP model are described in the following sections. Details regarding the DP model parameters and calibration of the softening parameters of the concrete material are available in Kenawy et al. (2020), and calibration of the steel rebar buckling parameters is discussed in this work.

The dynamic properties of the column are heuristically assigned such that the structure approximately represents a single degree of freedom system with a first-mode period of 1.0 second. Initial-stiffness-proportional and mass-proportional Rayleigh damping was assigned to the models, with a damping ratio of 5% of the critical damping in the first mode, and 10% in the third mode. For the LP model, stiffness-proportional damping was assigned to the frame elements, and mass-proportional damping was assigned to the nodes, following the approach described in Ibarra (2004).

The modeled column is subjected to a dataset of near-fault ground motions in 2D nonlinear time-history simulations. The displacement at the top end of the column is monitored throughout the analysis, and the maximum drift ratio (maximum displacement divided by the length of the column) is the engineering demand parameter of interest in the analysis. Finally, a truncated incremental dynamic analysis (IDA) is performed to evaluate the collapse fragility of the structure predicted by each modeling approach, following the procedure outlined in FEMA P-58 (ATC 2018). The ground motion records used in the IDA are initially scaled to a common spectral intensity level corresponding to the first-mode period of the column. Then, the column is subjected to successively scaled versions of the ground motion records at eight different intensity levels, and the portion of the records which leads to collapse at each level is recorded. The maximum likelihood method and algorithm developed by Baker (2015) are used to fit a lognormal distribution to the analysis results and determine the median collapse capacity of the column predicted by each modeling approach.

3 Integral Nonlocal Beam-Column Element

The element proposed by Kenawy et al. (2018) is a two-dimensional Euler-Bernoulli beam which follows a displacement-based (stiffness-based) state determination approach, and is enriched with nonlocal section deformation variables. The nonlocal element formulation introduces spatial averaging to the deformation variables within a chosen length scale as follows:

$$\widetilde{f(x)} = \int_L \bar{w}(x,r)\, f(r)dr \tag{1}$$

where f(x) is the deformation variable being averaged, $\bar{w}(x,r)$ is a normalized weighting function that is typically Gaussian or bell-shaped, and L is the characteristic length scale over which the variable is averaged, and generally spans multiple elements. The averaging operation incorporates interactions between each section (or integration point) x and its neighboring sections r within the characteristic length L. The nonlocal section deformations $\tilde{\mathbf{e}}(x_i)$ are computed as follows:

$$\tilde{\mathbf{e}}(x_i) = \frac{\sum_{k=1}^{N} w_i(r_k)\, \mathbf{e}(x_k)\Omega_k}{\sum_{k=1}^{N} w_i(r_k)\, \Omega_k} \tag{2}$$

where $w_i(r_k)$ is the value of the weight function at integration point k, and Ω_k is the quadrature weight associated with integration point k, and N is the number of integration points. In the DP fiber-section model, the nonlocal section strains are used to calculate nonlocal axial strain variables associated with each fiber in the cross section, which are then used by the nonlocal constitutive models to advance the damage state of the material in the form of mesh-objective strain-softening. The complete derivation of the nonlocal element framework is presented in Kenawy et al. (2018).

The imposed characteristic length parameter may be interpreted to characterize the zone over which the strain-softening behavior is recorded in a laboratory experiment (i.e., the zone over which the damage is represented in a smeared sense). The calibration of the characteristic length for the concrete material was discussed in Kenawy et al. (2020) but remains a topic of further study.

4 Constitutive Models

4.1 Nonlocal steel model formulation

The nonlocal steel model utilized in the present study is described herein. For the chosen model, the axial stress σ is computed from the following expression:

$$\sigma = \langle \sigma^e \rangle - (1-D)\langle -\sigma^e \rangle \tag{3}$$

where $D \in [0,1]$ is a nonlocal damage parameter, σ^e is the effective axial stress in the absence of damage, and $\langle \cdot \rangle$ denotes the Macaulay bracket (ramp) function, specifically:

$$\langle x \rangle = \begin{cases} 0, & x < 0 \\ x, & x \geq 0 \end{cases} \tag{4}$$

Only the compressive response of the model is affected by the evolution of damage, and is intended to emulate the softening behavior associated with buckling of the steel reinforcement due to lack of confinement.

The effective stress is updated independently of the damage parameter, and assumes the form of a conventional uniaxial plasticity model, namely:

$$\sigma^e = E(\varepsilon - \varepsilon^p) \tag{5}$$

where E is the elastic modulus, ε is the local strain in the material, and ε^p is the local measure of plastic strain. Linear kinematic hardening behavior is assumed, such that the model obeys the following yield constraint equation:

$$f_y = \left|\sigma^e - E^p\varepsilon^p\right| - \sigma_{y0} \leq 0 \tag{6}$$

where E^p denotes the plastic hardening modulus, and σ_{y0} is the initial yield stress. For the chosen yield function, the plastic strain is updated according to:

$$\varepsilon^p = \varepsilon^{p,tr} + \Delta\varepsilon^p n^{p,tr} \tag{7}$$

In the above, $\varepsilon^{p,tr}$ represents the initial trial value for the total plastic strain, $n^{p,tr}$ is the direction of plastic flow, i.e.

$$n^{p,tr} = \mathrm{sign}\left(\sigma^{e,tr} - E^p\varepsilon^{p,tr}\right) \tag{8}$$

and the plastic strain increment $\Delta\varepsilon^p$ is computed directly via:

$$\Delta\varepsilon^p = \frac{\langle f_y^{tr} \rangle}{E + E^p} \tag{9}$$

where f_y^{tr} denotes the trial value of the yield function evaluated using $\varepsilon^{p,tr}$.

The damage parameter is presumed to depend directly upon the nonlocal strain $\tilde{\varepsilon}$, which is essential to prevent strain localization. The damage parameter is assigned an initial value of zero corresponding to an initially undamaged state, and is updated according to the following expression:

$$D = \max\left\{D^{tr}, \tanh\left(\frac{-\tilde{\varepsilon}-\varepsilon_0^d}{\varepsilon_{3/4}^d-\varepsilon_0^d}\right)\right\} \tag{10}$$

where D^{tr} is the previous/trial value of the damage parameter, ε_0^d is the magnitude of the compressive strain at which damage initiates, and $\varepsilon_{3/4}^d$ is the nominal magnitude of compressive strain at which the damage reaches a value of $D = \tanh(1.0) \approx 3/4$. The chosen form of the above equation ensures that $D < 1.0$, such that the model retains some residual compressive strength to avoid numerical issues associated with poor global solution convergence.

An example illustration of the hysteretic behavior of the model is shown in Figure 1. The model was parameterized using an elastic modulus of $E = 200.0$ GPa, a plastic hardening modulus of $E^p = 2.0$ GPa, and an initial yield stress of $\sigma_{y0} = 446.0$ MPa. These parameters were calibrated based upon available experimental data relevant to the present study.

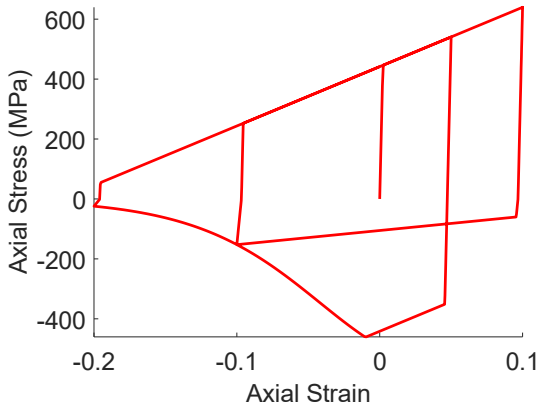

Figure 1. Hysteretic behavior of the proposed steel model under two increasing cycles of strain using the following model parameters: $E = 200.0$ GPa, $E^p = 2.0$ GPa, $\sigma_{y0} = 446.0$ MPa, $\varepsilon_0^d = 0.01$, $\varepsilon_{3/4}^d = 0.1$.

Appropriate calibration of ε_0^d and $\varepsilon_{3/4}^d$ depends on the context in which the proposed model is applied. Specifically, because the model is intended to represent the behavior of steel rebar within a RC column, the point at which buckling (represented as compressive damage) initiates and progresses will implicitly depend on the slenderness ratio of the rebar implied by the spacing of the transverse reinforcement, and the effects of confinement. The strain at which buckling (damage) initiates was presumed to coincide with the complete loss of confinement due to crushing of the surrounding concrete, which was estimated at ε_0^d=0.01. An effective buckling length was assumed to be equal to the nonlocal characteristic length of the model. The nonlocal steel buckling model developed by Kolwankar et al. (2017) was further used as a reference to guide the selection of the remaining steel softening parameters.

4.2 Nonlocal damage-plasticity concrete model

The uniaxial behavior of the concrete material is described by the nonlocal damage-plasticity model of Kenawy et al. (2020), in which the nominal axial stress σ_c is expressed as:

$$\sigma_c = (1-D_c)\, E_c(\varepsilon_c - \varepsilon_c^p) \tag{11}$$

where ε_c and ε_c^p are the total and plastic strains, respectively, and E_c is the elastic modulus. D_c is a damage parameter which can take on values between 0 (undamaged state) to 1 (fully damaged state). The damage

parameter controls both the strength and stiffness degradation of the material, and is evaluated as a function of a nonlocal version of a damage history variable k_{dc}: $D_c = D_c(\widetilde{k_{dc}})$, whose evolution is governed by the evolution of the nonlocal plastic strain. The complete details of the model are described in Kenawy et al. (2020). We use the same material parameters provided in the referenced article with respect to the compressive stress capacity, and conservatively assume that the material possesses no capacity to resist tensile stresses.

5 Database of Near-Fault Ground Motions

The dataset of near-fault ground motions was obtained from the PEER NGA-West2 database (Ancheta et al. 2014). It consists of 94 near-fault ground acceleration records, which were obtained by filtering the database for the following parameters: earthquake magnitudes between 6.7 and 7.4, Joyner Boore distance between 0 and 15 km, and V_{s30} between 200 and 700 m/s. The records used in this study are listed in Appendix 1 in Kenawy et al. (2023). The as-recorded horizontal component accelerations were rotated to their strike-normal (SN) and strike-parallel orientations based on the fault orientations extracted from the metadata of the record database. For brevity, we focus in this article on discussing the response of the structure to the SN horizontal component records only. The acceleration response spectra of those records are shown in Figure 2a.

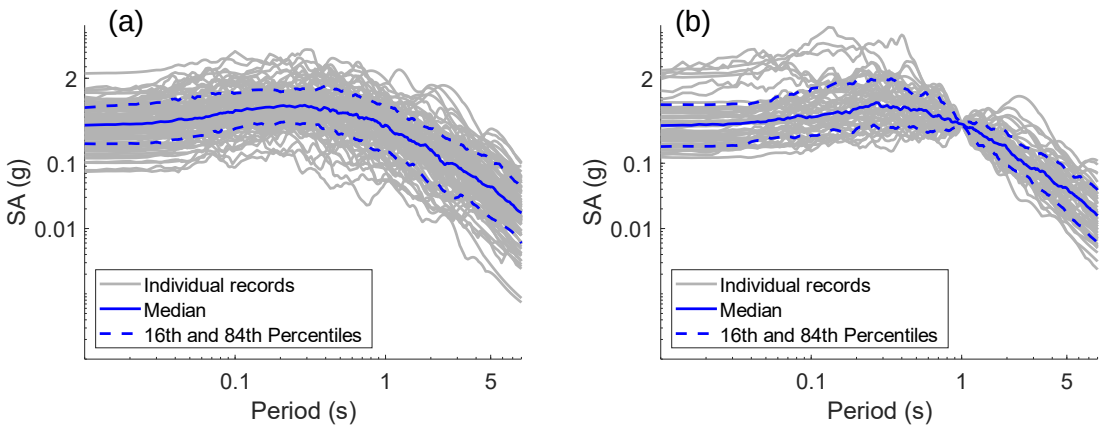

Figure 2: Acceleration response spectra associated with (a) the SN component near-fault ground motion records, and (b) a sample of the SN records scaled to a common spectral acceleration value at a period of 1.0 second.

For the purpose of the IDA, we randomly sample 50 records from the dataset, and scale them to a common intensity level (spectral acceleration) at the first-mode period of the structure. This initial value of the common intensity $SA(T_1)$ is not of importance to the study; therefore, we arbitrarily choose this value to be equal to the median $SA(T_1)$ of the sampled records. The scaled ground motion sample used for the IDA is shown in Figure 2b.

6 Results and Discussion

6.1 Quasi-static analysis

Figure 3 shows the deterioration of the lateral load-carrying capacity of the column under the influence of quasi-static lateral displacement cycles. Each subplot corresponds to one of the three alternative modeling approaches: the LP model, the Nonlocal DP Model, and the Local DP model. The response of the column to the same loading protocol recorded in the laboratory experiment is also shown in each subplot for the sake of comparison. As expected, the local model fails to appropriately predict the reduction in the lateral load-carrying capacity, because of the strain localization issues discussed previously. As a result, the lateral capacity of the column is severely underestimated by this modeling approach, compared to the reference recorded capacity. It is important to note that the load-displacement trace obtained in subplot (c) representing the local (or conventional) DP model is mesh-dependent, such that the post-peak slope changes substantially based on the number of elements used to model the column.

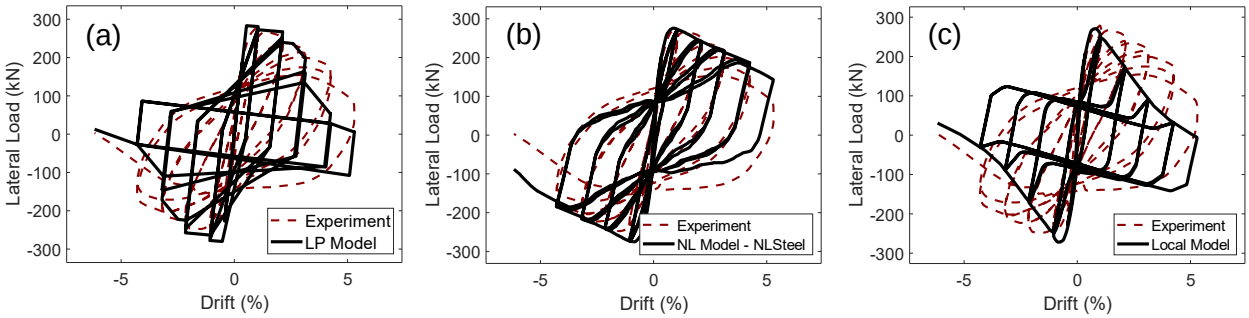

Figure 3: Lateral force vs. drift ratio predicted by: (a) the LP model, (b) nonlocal DP model, and (c) local DP model. The recorded observations in the reference laboratory experiment are shown in each subplot.

Comparing subplots (a) and (b) reveals that the initial reduction in the load-carrying capacity predicted by the nonlocal model is consistent with that observed in the experiment, whereas the LP model predicts more severe deterioration in the initial displacement cycles. However, in the final cycles of the test, the nonlocal model does not capture the severe deterioration in the capacity observed in the experiment, whereas the LP model more appropriately represents the deterioration of the column at the end of the test. It is worth noting that this particular column specimen is part of the database used to calibrate the parameters of the LP model in Haselton et al. (2016). Conversely, the calibration of the nonlocal model does not rely on any group of structural components. The predicted post-peak slope by the nonlocal model, however, depends on the value of the characteristic length associated with the nonlocal averaging. Details of the calibration of the nonlocal characteristic length are discussed in Kenawy et al. (2020), but we briefly demonstrate the sensitivity of the post-peak slope to the assigned value of the characteristic length: Figure 4 shows the load-displacement trace predicted by the nonlocal model for three different values of the characteristic length, which approximately correspond to 0.88 to 1.13 of the cross-sectional dimension of the column. Despite the relatively small change in the characteristic length value, the deterioration of the load-carrying capacity – especially in the final displacement cycles – is notably influenced by the variation of this parameter. Because of the form of the softening slope associated with the steel model, it is likely that the assigned characteristic length has a more pronounced effect on the buckling of the steel material, compared to the softening of the concrete material in the cross section, which takes a linear form. Current work by the authors examines the influence of the characteristic length in the presence of materials with different constitutive softening behavior in the cross section, but such an investigation is outside the scope of this study.

6.2 Nonlinear dynamic analysis

In this study, we define the collapse limit state to occur at a column drift ratio of 10%. This value was selected based on the general trends of the incremental dynamic analysis of the column. We first examine the seismic demands on the column imposed by ground motion records which did not result in collapse in any of the three models (i.e. those ground motions for which the predicted maximum drift ratio is less than or equal 10% in all three models); this dataset corresponds to 11 ground motion records only. Figure 5 shows the cumulative distribution of the maximum drift ratio of the column predicted by each model. Both an empirical cumulative distribution and a fitted lognormal distribution are shown for each case. The distributions shown in the figure suggest that the LP model may underestimate the demands on the column compared to the DP models, even for relatively low ground motion intensities. However, the differences between the distributions of the NL and LP models are not statistically significant, based on the Mann-Whitney U two-sample test (p-value = 0.79), which tests the null hypothesis that the data points in both samples come from distributions with equal medians. Similarly, the demands predicted by the nonlocal and local DP models are not significantly different, based on the same test (p-value = 0.95). The results shown in Figure 5 demonstrate the similarity of the structural demands predicted by each model at relatively low seismic intensity levels, and indicate consistency between the dynamic characteristics of each model.

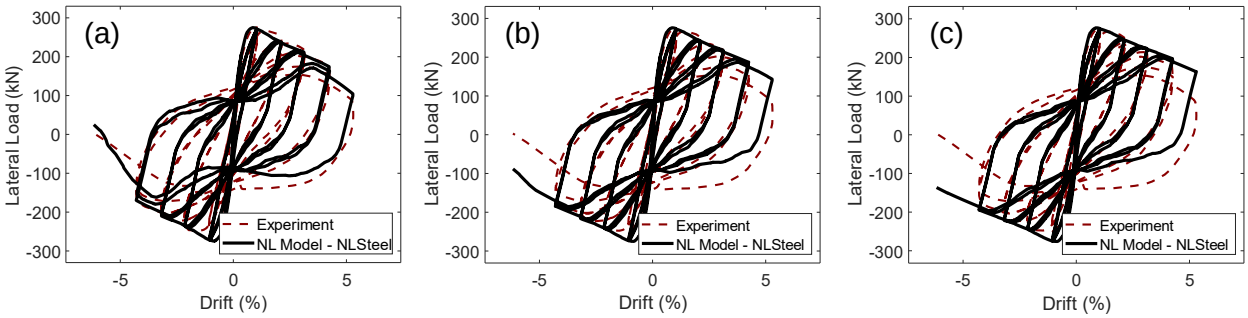

Figure 4: Lateral force vs. drift ratio predicted by the nonlocal DP model with three different characteristic length values: (a) L = 350 mm, (b) L = 400 mm, and (c) L = 450 mm. The recorded observations in the reference laboratory experiment are shown in each subplot.

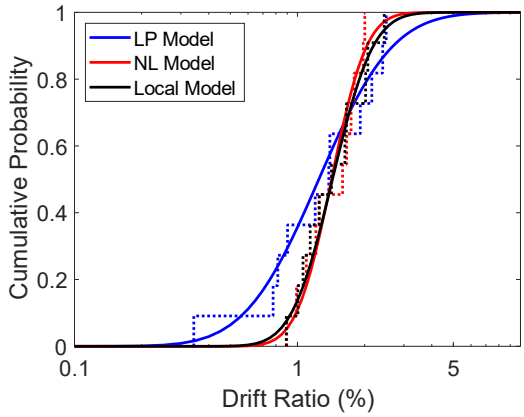

Figure 5: Cumulative distributions of the maximum drift ratio predicted by each model under the influence of 11 low-intensity ground motion records. Both an empirical (dotted lines) and a fitted lognormal distribution (solid lines) are shown.

6.3 Incremental dynamic analysis and assessment of collapse

The results of the truncated IDA are summarized using a collapse fragility distribution which defines the probability of the collapse of the structure at each spectral acceleration intensity level. The collapse fragilities of the column predicted by all three modeling approaches are shown in Figure 6. In contrast to the distributions of the demands imposed by low-intensity ground motions, substantial differences are observed between the collapse fragilities predicted by each model. For example, the median collapse capacity (expressed as a spectral acceleration value) predicted by the LP model is approximately three times the median capacity predicted by the nonlocal model. This observation suggests more severe deterioration associated with the nonlocal model when compared against the LP model. For example, at the highest $SA(T_1)$ value used in this study, the LP model predicts that only 41% of the ground motions lead to collapse, whereas the nonlocal model predicts that 98% of the ground motions lead to collapse. There are several potential reasons for this difference. First, both model types were not empirically calibrated under dynamic loading conditions; therefore, their expected performance under severe dynamic loading conditions is not well-constrained. However, the predictions of the nonlocal model fundamentally rely on uniaxial constitutive relationships associated with the steel and concrete materials. Therefore, its aggregated behavior is less vulnerable to calibration deficiencies than the LP model which is calibrated using full beam and column specimens with various cross-sectional properties. Second, the moment-rotation relationship of the LP model is modified to account for the interaction between the axial force and moments experienced by the column only in the initial calibration of the model parameters, whereas such effects are captured at each analysis time step in the nonlocal model. Consequently, the P-Delta effects predicted by each modeling approach may be substantially different. In addition, the change in the dynamic characteristics of the column due to yielding and localized deterioration effects changes its effective natural vibration period and the range of frequencies in each ground motion to which the column is sensitive. In other words, the different yielding behavior observed in the nonlocal and LP models may lead to each model experiencing different ground motion intensities at the same nominal intensity level. The predicted collapse fragility by the local DP model is also shown in Figure 6 only for reference. This

prediction exhibits spurious dependence on the chosen mesh size; therefore, the local model is not recommended for evaluating the collapse capacity of structures.

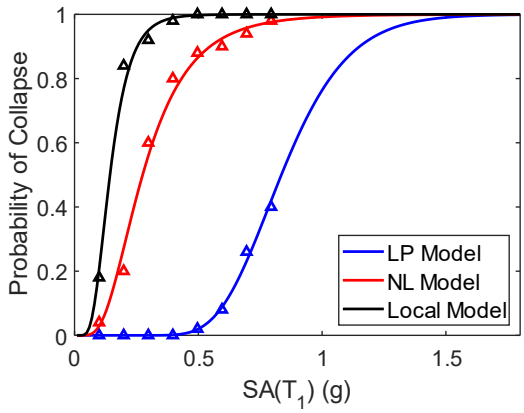

Figure 6: Collapse fragility of the column predicted by each model using a maximum likelihood fit. The fraction of collapse cases at each intensity level is also shown for each model type.

7 Conclusions

In this study, we created a numerical model of a RC column using three different modeling approaches, and assessed its performance under quasi-static and dynamic earthquake loading conditions. The findings of this study highlight the substantial modeling uncertainty associated with frame element models that may be used to evaluate the seismic demands on structures in a performance-based design context. We find that the predicted seismic demands on the RC column by all modeling approaches are not significantly different under relatively low-intensity ground shaking. However, substantial differences arise between the collapse fragilities of the column predicted by each model. The observed differences may be interpreted as an example of the extent of the modeling uncertainty associated with the lumped plasticity model, and a regularized version of the fiber-based distributed-plasticity model that is not sensitive to the finite element mesh size. We initially attribute the variations in the predicted collapse fragility between the nonlocal and LP models to differences in the calibration conditions of each model, which result in different deterioration patterns under dynamic loading, and alter the sensitivity of the structural component to the imposed ground motions. Current work by the authors explores the sensitivity of the predicted collapse capacity to the various modeling parameters in each case. In addition, future work will examine the influence of the wide record-to-record variability in this near-fault ground motion dataset (compared to a far-field dataset with narrower variability) on the collapse fragility predicted by each modeling approach.

8 References

Ancheta, T. D., Darragh, R. B., Stewart, J. P., Seyhan, E., Silva, W. J., Chiou, B. S.-J., Wooddell, K. E., Graves, R. W., Kottke, A. R., Boore, D. M., et al. (2014). NGA-West2 database. *Earthquake Spectra*, 30(3):989–1005.

ATC (Applied Technology Council) (2009). Quantification of building seismic performance factors (FEMA P-695). Washington, DC: US Dept. of Homeland Security, FEMA.

ATC (Applied Technology Council) (2018). Seismic Performance Assessment of Buildings (FEMA P-58). Washington, DC: US Dept. of Homeland Security, FEMA.

Baker, J. W. (2015). Efficient analytical fragility function fitting using dynamic structural analysis. *Earthquake Spectra*, 31(1), 579-599.

Bažant, Z. P., and T. B. Belytschko (1985). Wave propagation in a strain softening bar: Exact solution. *Journal of Engineering Mechanics*, 111 (3): 381–389. https://doi.org/10.1061/(ASCE)0733-9399(1985)111:3(381).

Bažant, Z. P., and F. Lin (1988). Nonlocal yield limit degradation. *International Journal for Numerical Methods in Engineering*, 26 (8): 1805–1823. https://doi.org/10.1002/nme.1620260809.

Bažant, Z. P., and M. Jirásek (2002). Nonlocal integral formulations of plasticity and damage: Survey of progress. *Journal of Engineering Mechanics*, 128 (11): 1119–1149. https://doi.org/10.1061/(ASCE)0733-9399(2002)128:11(1119).

Bertero, V. V., Mahin, S. A., & Herrera, R. A. (1978). Aseismic design implications of near-fault San Fernando earthquake records. *Earthquake Engineering & Structural Dynamics*, 6(1), 31-42.

Champion, C., & Liel, A. (2012). The effect of near-fault directivity on building seismic collapse risk. *Earthquake Engineering & Structural Dynamics*, 41(10), 1391-1409.

Chopra, A. K., & McKenna, F. (2016). Modeling viscous damping in nonlinear response history analysis of buildings for earthquake excitation. *Earthquake Engineering & Structural Dynamics*, 45(2), 193-211.

Coleman, J., and E. Spacone (2001). Localization issues in force-based frame elements." *Journal of Structural Engineering*, 127 (11): 1257–1265. https://doi.org/10.1061/(ASCE)0733-9445(2001)127:11(1257).

Feng, D. C., Chen, X., McKenna, F., & Taciroglu, E. (2023). Consistent Nonlocal Integral and Gradient Formulations for Force-Based Timoshenko Elements with Material and Geometric Nonlinearities. *Journal of Structural Engineering*, 149(4),04023018.

Giberson, M. F. (1967). The response of nonlinear multi-story structures subjected to earthquake excitation. California Institute of Technology, Pasadena, CA.

Hall, J. F., Heaton, T. H., Halling, M. W., & Wald, D. J. (1995). Near-source ground motion and its effects on flexible buildings. *Earthquake spectra*, 11(4), 569-605.

Haselton C. B., Liel A. B., Taylor-Lange S. C., Deierlein G. G. (2016). Calibration of model to simulate response of reinforced concrete beam-columns to collapse. *ACI Structural Journal*,113(6):1141-1152.

Ibarra, L. F. (2004). Global collapse of frame structures under seismic excitations. Stanford University.

Ibarra L. F., Medina R. A., Krawinkler H. (2005). Hysteretic models that incorporate strength and stiffness deterioration. *Earthquake Engineering and Structural Dynamics*, 34(12):1489-1511.

Kenawy, M., Kunnath, S., Kolwankar, S., & Kanvinde, A. (2018). Fiber-based nonlocal formulation for simulating softening in reinforced concrete beam-columns. *Journal of Structural Engineering*, 144(12), 04018217.

Kenawy, M., Kunnath, S., Kolwankar, S., & Kanvinde, A. (2020). Concrete uniaxial nonlocal damage-plasticity model for simulating post-peak response of reinforced concrete beam-columns under cyclic loading. *Journal of structural engineering*, 146(5), 04020052.

Kenawy M. & McCallen D. (2021) CCEER-20-07: Regional-scale seismic risk to reinforced concrete buildings based on physics-based earthquake ground motion simulations. Technical report, Center for Civil Engineering Earthquake Research, University of Nevada, Reno, NV.

Kenawy, M., McCallen, D., & Pitarka, A. (2021). Variability of near-fault seismic risk to reinforced concrete buildings based on high-resolution physics-based ground motion simulations. *Earthquake Engineering & Structural Dynamics*, 50(6), 1713-1733.

Kenawy, M., McCallen, D., & Pitarka, A. (2023). Characteristics and selection of near-fault simulated earthquake ground motions for nonlinear analysis of buildings. *Earthquake Spectra*, 39(4), 2281-2322.

Kolwankar, S., Kanvinde, A., Kenawy, M., & Kunnath, S. (2017). Uniaxial nonlocal formulation for geometric nonlinearity–induced necking and buckling localization in a steel bar. *Journal of Structural Engineering*, 143(9), 04017091.

McKenna, F., Fenves, G. L., Scott, M. H., et al. (2000). Open system for earthquake engineering simulation. University of California, Berkeley, CA.

Sideris, P., & Salehi, M. (2016). A gradient inelastic flexibility-based frame element formulation. *Journal of Engineering Mechanics*, 142(7), 04016039.

Soesianawati, M. T. (1986). Limited ductility design of reinforced concrete columns. Department of Civil Engineering, University of Canterbury.